

## **EXTRACTION OF FLOOD MASKS USING SATELLITE BASED VERY HIGH RESOLUTION SAR DATA FOR FLOOD MANAGEMENT AND MODELING**

S Voigt<sup>1</sup>, S Martinis<sup>1</sup>, H Zwenzner<sup>1</sup>, T Hahmann<sup>1</sup>, A Twele<sup>1</sup>, and T Schneiderhan<sup>1</sup>

1. German Remote Sensing Data Center, German Aerospace Center, Oberpfaffenhofen, 82234 Wessling, Germany

**ABSTRACT:** Demand for crisis information on natural disasters like severe flood events has increased substantially during recent years worldwide and especially in Europe. Simultaneously, a rising awareness of the availability of satellite information has led to an increase in requesting the corresponding mapping services. Because of their specific illumination and their all weather capabilities Synthetic Aperture Radar (SAR) sensors are optimally suited for providing reliable information on extensive floods, which usually occur under rainy or at least cloudy conditions. Flood information is needed as quickly as possible to provide an overview of the situation and to improve the crisis management and response activities. Analysing regularly acquired images floods can be monitored, which represents a valuable input for subsequent flood modelling techniques. In this paper an overview of the use of SAR for flood mapping is given and first experiences using the very high resolution satellite system of TerraSAR-X as well as key processing elements and some of the important analysis techniques used for the extraction of flood information are presented. Furthermore, value adding and flood parameter derivation principles are presented and examples of recent floods in Europe (United Kingdom, 2007) are shown, for which first TerraSAR-X data were analysed. Finally, a conclusion and outlook to the future prospects of high resolution SAR missions for flood mapping and monitoring is given.

Key Words: Satellite, SAR, Radar, Flood Extent, Mapping, high resolution.

### **1. INTRODUCTION**

Over the past years airborne and space borne synthetic aperture radar (SAR) systems have increasingly been used for mapping and monitoring of hydrological parameters. The most popular of these parameters is the flood extent. Especially with the operationally and routinely available space borne systems like ERS-1/2, Envisat, Radarsat, etc. very powerful systems were (and partially still are) available to map flood situations in the C-Band (~ 5 cm) domain. With the Shuttle Radar Missions SIR A/B, X-SAR SIR-C and the Shuttle Radar Topography Mission (SRTM) also L-Band (23 cm) and X-Band (3 cm) observations, including different polarization modes became possible from space during the operation of the missions and within range of the respective Space Shuttle orbits. From the data of those missions the backscatter characteristics and mapping capabilities with respect to the different features of water surfaces could be studied (e.g. Miranda *et al.*, 1997). The ALOS PALSAR sensor provides the possibility to study and map

water features in the L-Band and including the different polarization modes (HH, VV, VH and HV) from a polar orbiting platform. With the successful launch and commissioning of TerraSAR-X a new class of space based SAR systems suitable for flood monitoring became available for the scientific community in the X-Band domain and in the one meter pixel spacing class. Further systems like COSMO-SkyMed (meter-class, X-Band) and Radarsat-2 (three meter class, C-Band) are to follow soon.

As SAR systems in general have good cloud penetration capabilities they are often the preferred tool to observe flood situations from space, as these often occur during long lasting precipitation and cloud cover periods which, in many cases, hinder an observation by optical imaging instruments. The new class of high resolution meter class SAR sensors offers great potential in the field of flood mapping; however, also new challenges for processing and analysis arise from these images. While availability of three systems in orbit increases the repetition rate and observation frequency strongly, the high spatial resolution of the systems results in large variety of image objects and poses new problems for image analysis. This is especially the case for areas where single strong scatterers dominate the radar reflection and make the imagery difficult to be analyzed, as it is the case for example in urban areas (Solbø *et al.*, 2004). Especially in complex imaging scenarios such as highly structured built-up areas, the spatial resolution of classical space based SAR systems is too low for deriving flood perimeters with sufficient accuracy. Furthermore, also the SAR signal in the X-Band at 3 cm wavelength shows sensitivity to certain wave patterns induced by wind or heavy rain on the water surface. Water surfaces, under standard (calm) conditions, appearing black in a radar image suddenly turn out to be of strong scattering character. Also flood areas covered, even if only partially, by vegetation have different scattering properties in X-Band to those observed in C-Band (Townsend *et al.*, 2002; Wang *et al.*, 1995). New approaches have to be found to reliably identify water bodies in these high resolution SAR images. Object based, as well as pixel based methods have been developed (e.g. Horritt *et al.*, 1999; Ahtonen *et al.*, 2004; Heremans *et al.*, 2003) and need to be further refined for these purposes. Apart from these challenges of image classification, the high geometric accuracy and the repeated observation possibilities provide good options for the derivation of precise flood parameters like flood duration or flood dynamics. If further combined with geo information layers like high resolution digital elevation data of the river basis, the flood depth can quite well be estimated from these imagery.

## 2. A NEW SENSOR CLASS – TERRASAR-X CHARACTERISTICS

Although current spaceborne C-band SAR platforms have already demonstrated their usefulness for large-scale flood mapping in a number of cases, they can only provide spatial and temporal resolutions that make a detailed and near-real-time assessment of floods hardly feasible. Hence, medium resolution C-band SAR data have only seen a limited use for the operational assessment of large area flood situations. In most cases, the low repetition rate typically only allows a single SAR data acquisition per flood event, at best, with an even lower probability to depict the maximum water level.

The German TerraSAR-X satellite was launched on 15 June 2007 from the Baikonur Cosmodrome in Kazakhstan, into a 514 km high, sun-synchronous and near-polar dusk-dawn orbit. While the nominal repetition rate of the satellite is 11 days, each point of the Earth can be targeted within two to four days depending on its latitude using a large variety of different look angles. The possibility to rotate the satellite system for an experimental left-looking mode can further accelerate acquisition times, which is particularly important in the context of disaster mapping and monitoring.

The active antenna of TerraSAR-X allows the following imaging methods to be used: a) In the **SpotLight** (SL) and **High Resolution SpotLight** (HS) modes, a pixel spacing between 1 and 2 meters can be achieved. Depending on the mode selection (SL or HS), the size of the ground track is either 5x10 or 10x10 km. Although both modes are very similar, the HS mode increases the geometric resolution in azimuth at the expense of azimuth scene extension. b) In the **StripMap** (SM) mode, TerraSAR-X images a strip of 30 km width and maximum length of 1500 km. Depending on the incidence angle and processing options, the pixel spacing can be up to 3 meters. c) The **ScanSAR** mode (SC) combines four adjacent sub-swaths with quasi-simultaneous beams to a total swath width of 100 kilometers and maximum length of 1500 km at a pixel spacing of 16 meters.

For each imaging mode, a plethora of different acquisition parameters can be defined (incidence angle, polarization, look direction, processing parameters), which makes the SAR very versatile and adaptable to different application requirements.

In addition to TerraSAR-X, the Cosmo-SkyMed satellite system will provide X-band SAR data with similar characteristics. Cosmo-SkyMed is a system comprising a final configuration of four medium-sized satellites. As the first two satellites have already been successfully launched in June and December 2007, the possibility of observing an area of interest with a high temporal and spatial resolution has increased considerably. Together with the upcoming launch of the remaining two Cosmo-SkyMed satellites in 2008 and 2009, as well the new Radarsat-2 satellite, operating at C-band, a considerable number of spaceborne SAR systems will become available that will allow for rapid response times in order to map flood events at near-real-time. In conclusion, the advent of these high resolution X-band SAR satellites dramatically increases the potential to detect water in complex, local monitoring scenarios and potentially fosters the application of satellite SAR imagery in the context of a rapid flood mapping and detailed post-disaster damage assessment.

### **3. DERIVATION OF FLOOD MASKS FROM HIGH RESOLUTION SAR-SENSORS**

#### **3.1 Different backscatter characteristics of water in high resolution SAR data**

The availability of high resolution TerraSAR-X satellite imagery allows the image interpreter to distinguish more feature details on the earth's surface. Even waves with a wavelength in the range of the sensor resolution, of up to 1 m, may be visible as bright linear features on the surface of lakes or the sea. Texture analysis may be useful to use these regular features to classify them as water bodies. Vegetation standing within a water body may also increase the backscatter values, which in turn leads to regions that appear brighter than regular surfaces of water bodies. The use of dual polarization data can help to distinguish between dry surfaces, vegetation under water and standard water bodies. In built up areas it is often difficult to distinguish between radar shadow areas and water bodies, which both appear dark. In the context of flood situations, the improved pixel spacing of high resolution TerraSAR-X data potentially helps to map the inundated urban areas more reliably, although the limitations in very small-scaled scenarios also need to be assessed carefully.

Figure 1 shows various potential backscatter characteristics of water bodies: Rivers are not very susceptible to wind induced waves due to their small width and hence appear predominantly dark in SAR data. If the flow velocity and the river dynamic increases and therefore the river surfaces become rougher and more turbulent, this as well can lead to higher backscatter values. This effect can be seen in the TerraSAR-X example of the Rhine Falls waterfall. Although X-Band radar waves are claimed to be independent of atmospheric disturbances there can be situations with heavy thunderstorms containing big raindrops which may influence the radar image. Such an event can be seen in the Louisiana TerraSAR-X image as a dark veil. High mountainous terrain with steep slopes may cause radar shadow when the SAR data is acquired at shallow incidence angles. Auxiliary data like the SRTM digital elevation model can be utilized to distinguish between the dark radar shadow western slopes and the dark water surface of Lake Lucerne in the Swiss Alps. Another problem for the automatic classification of water bodies are man-made obstacles like fish farming basins, ships or bridges with ghost effect caused by multiple reflections at the bridge and the water surface, which can be seen in the SAR image of the coast of Portugal.

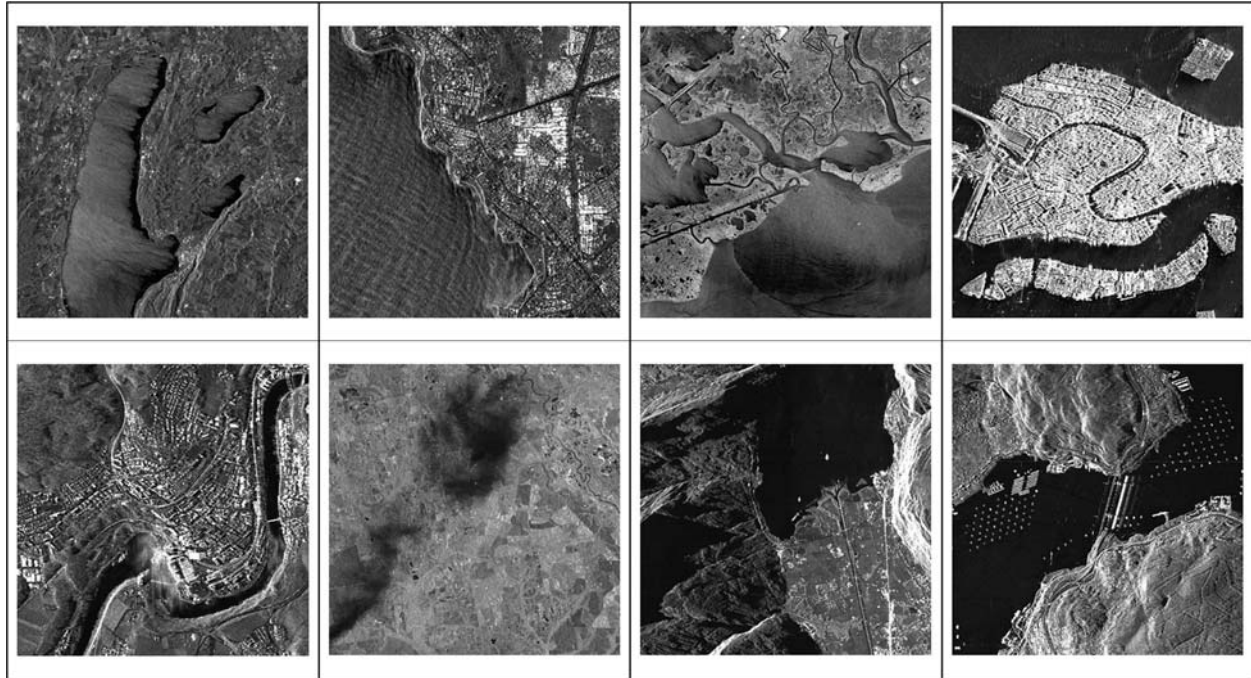


Figure 1: Different forms of appearance of water bodies in TerraSAR-X data, © DLR (2007, 2008) - from left to right, and top to down: Wind pattern on Lake Ammersee (Germany), reflected waves at Dakar coast (Senegal), Mississippi Delta wetlands (USA), urban area water bodies in Venice (Italy), turbulent water surface at the Rhine Falls waterfall (Switzerland), heavy rain/waterdrops in Louisiana (USA), radar shadow at the western slopes of Lake Lucerne (Switzerland), obstacles like a bridge with ghost effect and fish farming basins near Vigo (Portugal)

### 3.2 Comparison of Pixel-Based and Object-Based Approaches

Pixel-based and segmentation-based classification techniques can be distinguished as the two main concepts for the identification of flooded areas in radar imagery (Heremans *et al.*, 2003). Traditional classification approaches use pixels as smallest geometrical components of raster data. The gray values of the pixels which correspond to the spectral properties of a target can be used to group the image information into different semantic classes. Routinely, these approaches are widely applied to low and medium resolution remote sensing data. However, parameters for the classification are limited. Additionally, pixel-based classifiers do not make use of spatial information of the image and thus are not suited to deal with the inherent heterogeneity within land-cover units. Furthermore, even if noise reduction by speckle filtering is applied, classification results usually suffer from a salt-and-pepper effect and a post-processing classification by filtering becomes necessary. These smoothing methods however work without considering the original information.

By the use of image segmentation techniques, some problems of pixel-based image analysis can be solved. The created homogeneous, non-overlapping segments have a strong correlation with real objects or areas of the earth's surface. Image segmentation methods become more and more important in the field of remote sensing image analysis – in particular due to the increasing spatial resolution of imagery. Especially for data of the new generation of very high resolution optical and SAR sensors with a geometrical resolution of less than 1 m the use of segmentation-based methods appears promising. A disadvantage of this technique is the high processing demand of the segmentation step, which mostly limits the size of the processed image.

Thresholding is one of the most frequently used techniques to separate flooded from non-flooded areas in a SAR image (e.g. Townsend *et al.*, 1998; Brivio *et al.*, 2002). Commonly, classification is performed by assigning all elements of the SAR intensity data with a lower scattering cross-section than a given threshold to the flood class. One of the main advantages of this classification method is that it is computationally relatively inexpensive and therefore suitable for rapid mapping purposes. Its results are reliable and commonly, most of the extent of an inundation area can be derived by this technique. Thresholding works satisfactory for calm water surfaces, which can be regarded as specular reflectors with low backscatter values for the used radar wavelengths. In contrast, the surrounding terrain exhibits higher signal return due to strengthened surface roughness. The applied threshold will depend on the contrast between the water and land classes as well as on the deviation of the flood area from a smooth surface due to influences of wind induced waves, precipitation as well as of diffuse and corner reflecting vegetation.

Given this drawback, active contour models (e.g. Williams and Shah, 1992; Horritt *et al.*, 1999) have recently gained popularity as a means of finding smooth boundaries from incomplete and noisy images using local tone and texture measures. These “snake” algorithms had been used by e.g. Ahtonen *et al.* (2002), Horritt *et al.* (2001) and Matgen *et al.* (2007) for flood boundary delineation in medium resolution SAR imagery. Thus, flooded areas are identified as regions of homogeneous speckle statistics. Due to the fact that originally the snake has to be initialized manually for each water area, too much user input is required to extract flood masks from very high resolution SAR imagery on which large inundation areas mostly are divided into numerous flooded parcels. Therefore, approaches approximating the numerous flood areas by thresholding and transferring these initial polygons to the active contour algorithm appear more promising (Heremans *et al.*, 2003). However care must be taken initializing the algorithm both manually and automatically.

In most cases, multi-temporal analysis has proven superior to single data approaches. However, in rarest cases reference data are available for the respective flood area. Different change detection approaches for the derivation of flood dynamics between registered SAR data have successfully been applied in the past. These include amplitude based (e.g. Townsend *et al.*, 1998; Heremans *et al.*, 2003) as well as coherence based techniques derived from the use of C-Band SAR interferometry (e.g. Geudtner *et al.*, 1996; Dellepiane *et al.*, 2000; Nico *et al.*, 2000). However, at the moment repeat-pass X-Band SAR interferometry is not very suitable for mapping flood areas due to the strong temporal signal de-correlation during the repetition period of 11 days of TerraSAR-X. In the near future this method will become more interesting due to the upcoming short temporal baseline interferometric SAR systems of the TerraSAR-X and COSMO-SkyMed tandem missions. Using amplitude change detection in combination with C-Band multi-temporal SAR imagery, areas of flooded dense vegetation were mapped successfully e.g. by Townsend *et al.* (2002). This arises from the fact that microwaves at longer wavelengths can penetrate the forest canopy and are double bounced at the smooth water layer and the forest stems which causes a significant increase in backscatter.

#### **4. DERIVATION OF FLOOD RELATED PARAMETERS**

For the purpose of flood risk and flood damage assessment, other flood related parameters than flooded area such as inundation depth and flood duration are required. Since these parameters can not be derived directly from satellite data, additional information has to be included.

The factor which is of most concern with respect to damages caused by flooding is water depth. A standard approach for the estimation of direct physical damages to housing and property are stage-damage-functions for different building types or building uses (Thieken *et al.*, 2005). Hence, damages measured in monetary loss can be described and modeled as a function of water depth. Other more complex damage modeling approaches also include the duration of floods and flow velocity. The latter has to be seen as the major damage factor in case of flash flood situations especially on smaller rivers. Apart from flow velocity which can only be estimated by hydraulic models, remote sensing has the potential to derive flood depth and flood duration with a very high spatial resolution compared to hydraulic approaches. In addition, remote sensing based approaches can be valuable for the validation and verification of hydraulic model parameters.

#### 4.1 Flood depth

The derivation of inundation depth requires the incorporation of a high resolution digital terrain model (DTM). DTMs from LIDAR with 1-2 meters pixel resolution and 0.1 meter height accuracy are nowadays available for many river flood plains and have been satisfactorily used for hydrological applications and for the purpose of flood depth assessment. Promising methods of the latter are presented by Matgen *et al.* (2007) and Bates *et al.* (2006). A raster layer of flood depth can be derived by subtracting the terrain elevation from the elevation of the water surface. For the derivation of the flood water surface elevation the flood mask must be interlinked with the terrain data. Figure 2 (left) depicts the elevation of certain points on the flood boundary showing several variations and irregularities due to classification errors or location discrepancies between the DTM and the flood mask. Several correction steps have to be applied. As shown in figure 2 (right) this can be done by drawing cross-sectional profiles which connect the left and right river banks. According to these profiles the flood mask boundary can be adjusted (shifted) and rectified to the terrain model in order to generate a “smooth” water surface layer from which a TIN (triangular irregular network) can be derived.

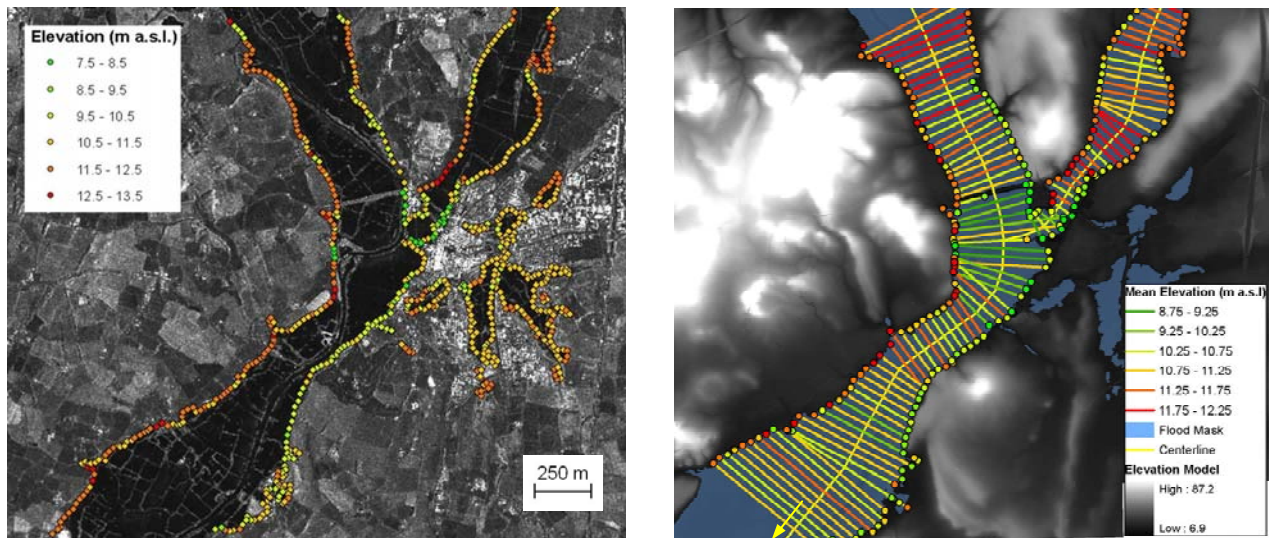


Figure 2: Left: TerraSAR-X image of the flood situation of July 25, 2007, at the River Severn near Tewkesbury, UK. The elevation of the borderline of the flooded area was extracted from an elevation model and drawn as colored points. Right: Cross-sectional profiles with a distance of 100 meters at the centerline of the river. The profile color represents the mean elevation of the left and right river bank. Problems and irregularities can be identified in built-up urban areas close to the river junction.

#### 4.2 Duration and Dynamics

Generally, the great advantage of SAR satellite systems for assessing floods is due to their reliable and genuine spatial representation of the flood extent. However, the temporal delineation of floods is limited because one satellite data take is only a snapshot in time. The assessment of flood dynamics and flood duration from satellite data requires a number of data takes recorded on different time steps during the flood period. A common technique for displaying changes in flood extent between two or three SAR satellite scenes is the generation of a color-composite as shown in figure 3. In this technique the grey values of one image are reassigned to one of the three color channels blue, green or red. A certain color can then be attributed to changes in flood extent. In the future, multi-observation conditions can be fulfilled with the various operational high resolution SAR satellite systems (see chapter 2). Through the combined use of different satellites, a repetition rate of less than 12 hours can be achieved.

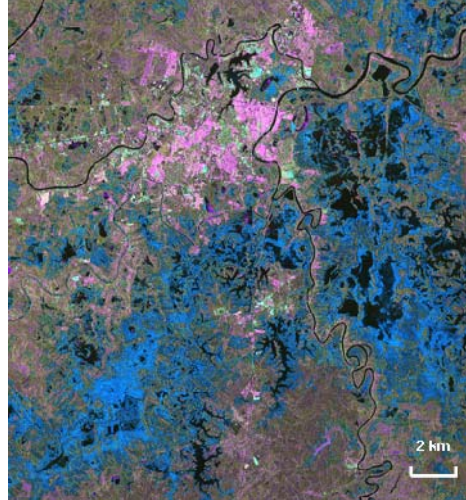


Figure 3: Color-composite of two TerraSAR-X scenes showing the flood situation around the city of Villahermosa/Mexico (shown in pinkish color) on Nov 8<sup>th</sup>, 2007 and the post-flood situation on Dec 2<sup>nd</sup>, 2007. The blue color stands for changes in flood extent and thus reflects flooded area. Areas which were inundated on both dates appear in black color.

## 5. CONCLUSION AND OUTLOOK

In this paper the advantages and challenges of the use of very high resolution SAR imagery for the analysis of flood situations could be shown. It can be concluded that the future of operational SAR mapping of floods is very positive, especially when looking at the currently launched space systems. Since many different parameters influence radar backscatter, the extraction of flood masks from X-band SAR data is not a trivial task. Robust methods need to be further developed to extract the water masks of inundated areas with high accuracy, but also as rapidly as possible. Such good and reliable availability of flood observations is of high relevance, especially during a flood disaster, when decision makers and relief organisations need a quick overview of the situation and detailed insights into the affected area in order to allocate their resources with maximum efficiency. With new possibilities in polarimetry, wavelength, spatial resolution and other characteristics given by the new available SAR sensors new approaches to extract the flood mask are currently being developed and need to be further automated and operationalized in order to improve the routine availability of space based flood monitoring to the extent possible.

**ACKNOWLEDGEMENT:** The authors would like to acknowledge the kind contributions to the work presented from the DLR-ZKI team, the TerraSAR-X project and the SAR working group of DLR-IMF. Most part of this work is funded by the BMBF research grant on the SAR-HQ project in the context of the BMBF-National Research Programme "Risk Management of Extreme Flood Events" (RIMAX).

## REFERENCES

- Ahtonen, P., Euro, M., Hallikainen, M., Solbø, S., Johansen, B., and Solheim, I. 2004. SAR and optical based algorithms for estimation of water bodies. Technical report, FloodMan Project, <http://projects.itek.norut.no/floodman>.
- Bates, P.D., Wilson, M.D., Horritt, M.S., Mason, D.C., Holden, N., and Currie, A. 2006. Reach scale floodplain inundation dynamics observed using airborne synthetic aperture radar imagery: Data analysis and modeling. *Journal of Hydrology* 328: 306-318.

- Brivio, P.A., Colombo, R., Maggi, M., and Tomasoni, R. 2002. Integration of remote sensing data and GIS for accurate mapping of flooded areas. *International Journal of Remote Sensing* 23(3): 429-441.
- Dellepiane, S., Bo, G., Monni, S., and Buck, C. 2000. SAR images and interferometric coherence for flood monitoring. In *Proc. of Geoscience and Remote Sensing Symposium (IGARSS '00)* 6: 2608-2610.
- Geudtner, D., Winter, R., and Vachon, P. 1996. Flood monitoring using ESR-1 SAR Interferometry coherence maps. In *Proc. of Geoscience and Remote Sensing Symposium (IGARSS '96)* 2: 966-968.
- Heremans, R., Willekens, A., Borghys, D., Verbeeck, B., Valckenborg, J., Acheroy, M., and Perneel., C. 2003. Automatic detection of flooded areas on ENVISAT/ASAR images using an object-oriented classification technique and an active contour algorithm. In *Proc. IEEE Conf. on Recent Advances in Space Technologies (RAST2003)*, pages 289-294, Istanbul, Turkey, November 20-22, 2003.
- Horritt, M.S. 1999. A statistical active contour model for SAR image segmentation. *Image and Vision Computing* 17: 213-224.
- Horritt, M.S., Mason, D.C., and Luckman, A.J. 2001. Flood boundary delineation from synthetic aperture radar imagery using a statistical active contour model. *International Journal of Remote Sensing* 22(13): 2489-2507.
- Matgen, P., Schumann, G., Henry, J.-B., Hoffmann, L., and Pfister, L., 2007. Integration of SAR-derived inundation areas, high precision topographic data and a river flow model toward real-time flood management. *Journal of Applied Earth Observation and Geoinformation* 9: 247-263.
- Miranda, F.P., Fonseca, L.E.N., Beisl, C.H., Rosenqvist, Å., and Figueiredo, M.D.M.A.M. 1997. Seasonal mapping of flooding extent in the vicinity of the Balbina Dam (Central Amazonia) using RADARSAT-1 and JERS-1 SAR data. In *RADARSAT for Amazonia: Results of ProRADAR Investigations*, edited by F. J. Ahern (Ottawa: Canada Centre for Remote Sensing, Natural Resources Canada), 187-191.
- Nico, G., Pappalepore, M., Pasquariello, G., Refice, A., and Samarelli, S. 2000. Comparison of SAR amplitude vs. coherence flood detection methods - a GIS application. *International Journal of Remote Sensing* 21(8): 1619-1631.
- Solbø, S., Pettinato, S., Paloscia, S., Santi, E., Brusotti, P., and Solheim, I. 2004. Mapping of flooding in the Alessandria area with ERS. In *Proc. of Geoscience and Remote Sensing Symposium (IGARSS '04)* 7: 4689-4692.
- Thieken, A.H., Müller, M., Kreibich, H., and Merz, B. 2005. Flood damage and influencing factors: New insights from the August 2002 flood in Germany. *Water Resour. Res.* 41(12): W12430.
- Townsend, P.A. and Walsh, S.J. 1998. Modeling flood plain inundation using integrated GIS with radar and optical remote sensing. *Geomorphology* 21(98): 295-312.
- Townsend, P.A. 2002. Relationships between forest structure and the detection of flood inundation in forest wetlands using C-band SAR. *International Journal of Remote Sensing* 23(3): 443-460.
- Wang, Y., Hess, L.L., Filoso, S., and Melack, J. M. 1995. Understanding the radar backscattering from flooded and non-flooded amazonian forests: results from canopy backscatter modelling. *Remote Sensing of Environment*, 54: 324-332.
- Williams, D.J. and Shah, M. 1992. A fast algorithm for active contours and curvature estimation. *CVGIP: Image Understanding* 55(1): 14-26.